

Learning Behavioral Representations from Wearable Sensors

NAZGOL TAVABI, USC Information Sciences Institute

HOMA HOSSEINMARDI, USC Information Sciences Institute

JENNIFER L. VILLATTE, University of Washington

ANDRÉS ABELIUK, USC Information Sciences Institute

SHRIKANTH NARAYANAN, University of Southern California

EMILIO FERRARA, USC Information Sciences Institute

KRISTINA LERMAN, USC Information Sciences Institute

The ubiquity of mobile devices and wearable sensors offers unprecedented opportunities for continuous collection of multimodal physiological data. Such data enables temporal characterization of an individual's behaviors, which can provide unique insights into her physical and psychological health. Understanding the relation between different behaviors/activities and personality traits such as stress or work performance can help build strategies to improve the work environment. Especially in workplaces like hospitals where many employees are overworked, having such policies improves the quality of patient care by prioritizing mental and physical health of their caregivers.

One challenge in analyzing physiological data is extracting the underlying behavioral states from the temporal sensor signals and interpreting them. Here, we use a non-parametric Bayesian approach, to model multivariate sensor data from multiple people and discover dynamic behaviors they share. We apply this method to data collected from sensors worn by a population of workers in a large urban hospital, capturing their physiological signals, such as breathing and heart rate, and activity patterns. We show that the learned states capture behavioral differences within the population that can help cluster participants into meaningful groups and better predict their cognitive and affective states. This method offers a practical way to learn compact behavioral representations from dynamic multivariate sensor signals and provide insights into the data.

ACM Reference Format:

Nazgol Tavabi, Homa Hosseinmardi, Jennifer L. Villatte, Andrés Abeliuk, Shrikanth Narayanan, Emilio Ferrara, and Kristina Lerman. 2022. Learning Behavioral Representations from Wearable Sensors. 1, 1 (June 2022), 16 pages. <https://doi.org/10.1145/nnnnnnn.nnnnnnn>

1 INTRODUCTION

Advances in sensing technologies have made wearable sensors more accurate and widely available, allowing for continuous and unobtrusive acquisition of multimodal physiological data, including heart rate, breathing, and physical activity. This data potentially allows for real-time, quantitative characterization of human behavior, which provides a basis to assess individual's health [3] and psychological well-being [51].

To make sense of physiological data, however, a number of challenges have to be solved. Sensor data is dynamic, very noisy, and often incomplete, with many missing values. Data streams coming from multiple sensors and individuals usually have very different time scales and cover different data collection periods. These characteristics make aggregating, reconciling, and modeling sensor data very challenging. Researchers have used Hidden Markov Models (HMMs) [37] to address some of these challenges and effectively capture temporal trends within physiological data [1, 35, 36, 44]. HMMs are a family of generative probabilistic models for sequential data in which the system can be represented as a Markov process with latent, or "hidden", states. These hidden states determine the dynamics of the process. One weakness of traditional HMMs is that they constrain the model to a predefined number of states. When learning dynamic behaviors from multiple physiological signals, it may be

difficult to enumerate the states best representing the data without making strong assumptions. Even with prior knowledge many variations in the signals, originated from environmental noise or artifacts in data collection, may change the distribution of underlying states and require more states.

To address this challenge, we propose to use a non-parametric Markov Switching Autoregressive model [16]—the *Beta Process Autoregressive HMM*—to learn shared latent states of data collected from wearable sensors. The number of states in this model is learned from the data: if an unusual new pattern appears in data, another state is added to model that segment. This is beneficial in cases where there is a malfunction or noise on the sensors. By assigning a separate state to that segment, we can be able to identify and disregard that state.

We apply the model to physiological data collected from about 200 workers at a large urban hospital. The workers agreed to participate in a 10 week-long study, during which they wore sensors that collected their bio-behavioral data. We show that the proposed model learns hidden states that correspond to shared behaviors of the workers, which provide useful features for behavioral modeling. We use these behavioral representations to better understand and analyze the data, group similar individuals together, and as features to predict their psychological traits, personality, and demographics. Using this framework, business owners can personalize each individual’s responsibilities depending on their identified clusters and estimated physical and psychological traits, in order to build a healthier and more productive workplace.

Our paper makes the following contributions:

- We learn shared behaviors from multivariate physiological data collected in the wild, i.e., from people going on about their daily lives, using BP-AR-HMM model.
- We use the learned shared states to define distance measures between participants, which are validated by clustering participants into meaningful groups.
- We propose
 - (1) A compact representation of participants to gain more insight into the data, interpret the learned latent states and find relations between different behaviors/states and individual attributes.
 - (2) A more advanced but less interpretable representation to predict individual attributes, such as personality traits, age, etc.

The rest of the paper is organized as follows. After reviewing relevant related work (§2), we describe the model (§3) Afterwards we describe the collected data (§4). Finally, we present results of our data analysis and prediction, and conclude with a discussion of their significance (§5).

2 RELATED WORK

Physiological data from wearable sensors have been used in a number of applications, most commonly for activity recognition. In such tasks, the goal is to learn the activity labels of each time unit (e.g. running, jumping, etc) based on their sensory data. Labels are usually collected in a controlled lab setting [16, 38]. In the case of in-the-wild studies, labels are either provided by real-time annotations of the user [4] or by human annotators when the study is over [46]. Another line of research attempts to predict users’ personality traits(e.g., degree of extraversion vs introversion), well-being and performance [23, 24] where the labels are collected from the participants as pre- or/and post- surveys. In this line of research the entire signal is analyzed to predict a final outcome which is different from activity recognition where the goal is to predict a label for each time unit.

In this work, since we do not have access to activity labels of participants at each time step, we use information from pre-study surveys, such as personality traits, to interpret the underlying behavioral states we learn from the physiological data. In other words, we use this framework to investigate possible correlations of learned behaviors (states) with certain personality traits. In the rest of this section, related methods in extracting behavioral states or features from physiological data are described.

Learning compact representations becomes especially important when dealing with physiological data. In these types of problems we usually don't have large number of participants however, for each participant we have rich longitudinal data. Since we have one label per data stream, participant, our training data is limited to the number of participants in the study, in this case 180 data points. Complex models, such as those learned by deep neural networks, tend to overfit on small training data, and thus are not applicable for these problems. In fact having rich data only increases the number of parameters needed to learn compact meaningful representations and hence increases the possibility of overfitting.

Piecewise Aggregate Approximation (PAA) [27] and *Symbolic Aggregate Approximation* (SAX) [31] are compact time series representations. PAA reduces a time series of length N to a representation of length W , by dividing the signal into W segments and replacing each segment by its average. SAX discretizes PAA representations into predefined letter sequences, symbolic representations aimed at replacing numerical time series with strings. Both PAA and SAX are dependant on the length of the time series, so signals with different lengths can not be compared using these representations.

Hidden Markov Models (HMMs) represent temporal trends and dynamics of time series using states and transition probabilities. Since transition probabilities are not time dependant, HMMs' parameters of time series with different lengths could easily be compared. In prior research, HMM models are learned on each time series independently [5]. As a consequence, the learned states cannot be compared across different representations. In addition to HMM models, other recent methods for temporal modeling suffer from the same shortcoming when applied to multiple signals: for example, the approach by Hallac et al. [20], which offers a new perspective on clustering subsequences of multivariate time series, cannot be used in learning representations across multiple signals. Another shortcoming of standard HMM models is that the number of states must be fixed a priori. Recent Bayesian approaches overcome these constraints by allowing infinitely many potential states using Beta process, which are shared among all time series [14–16]. This allows each time series to be represented in the space of shared latent states. This approach have successfully been applied to automatically capture different types of eye movements [25], human body motion [16] and understanding dynamics of forums in deep and darkweb[47]. There is another line of work which allows for infinite potential states in a Hidden Markov Model. Beal et al. [6] use the Dirichlet process [2] as prior over the hidden states, but the model is again designed to capture each time series independently.

Another approach in finding shared latent features among multiple time series is tensor decomposition. Tensor-based methods have been extensively used in different fields [29] including behavioral modeling [23, 24, 41]. A popular tensor decomposition method is Parafac2 [21], which offers multilinear higher-order decomposition that can handle missing values and different length time series. Parafac2 itself is considered a traditional method, however there are multiple works published in recent years on improving it's inference, imposing constraints, etc [10, 26]. Similarly a recent work by Wu et al. [55] proposes Random Warping Series (RWS), a model based on Dynamic Time Warping to find similarities between different length, multivariate time series and embed them in an N -dimensional space. This embedding technique was able to outperform state of the art methods in clustering and classification of time series. In this paper, we compare our results against RWS and Parafac2.

3 METHODS

3.1 Beta Process Autoregressive HMM

One of the most popular tools for studying multivariate time series is vector autoregressive (VAR) model [34]. In a VAR model of lag r , each variable is a linear function of itself and the other variable's r previous values. However, such models cannot describe time series with changing behaviors. In order to model such cases, Markov switching autoregressive models, which are generalization of autoregressive and Hidden Markov Models [34] are used.

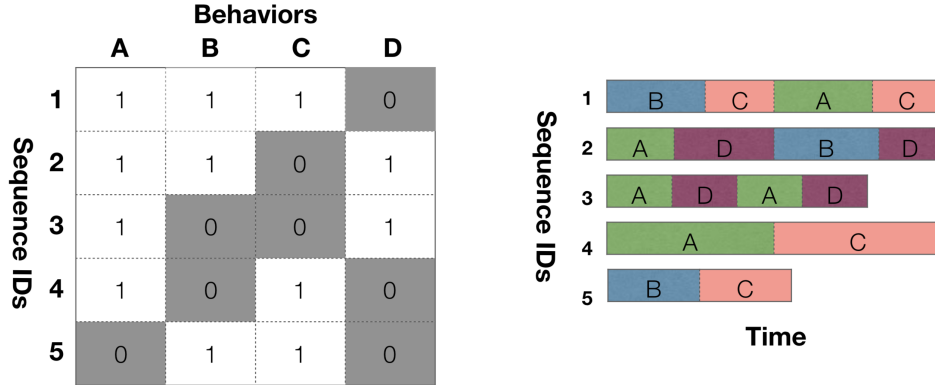


Fig. 1. Illustration of the model. Left image is matrix F . Based on this matrix time series 1 exhibits states A, B and C but there is a zero probability of time series 1 going into state D. The right image shows state sequences of time series

In this paper, we use a generative model proposed by [14, 16], called *Beta Process Autoregressive HMM* (BP-AR-HMM), to discover behaviors, or regimes of Markov switching autoregressive models that are shared by different time series. Based on the proposed model, the entire set of time series can be described by the globally-shared states, or behaviors, where each time series is associated with a subset of them. Behaviors associated with different time series can be represented by a binary matrix F , where $F_{ij} = 1$ means time series i is associated with behavior j . Given matrix F , each time series is modeled as a separate hidden Markov model with states it exhibits. An example of F matrix and the corresponding state sequences are shown in Figure 1

HMM is represented by a transition matrix T_i , which is a square matrix with dimensions equal to the number of states time series i exhibits. Entry $T_i(m, n)$ is the probability of transitioning from state m to state n for time series i , hence, the sum of each row equals to 1. Each state is modeled using a vector autoregressive process with lag r .

$$y_t = \sum_{l=1}^r A_{l,z_t} y_{t-l} + e_{z_t} \quad (1)$$

$$e_{z_t} \sim \mathcal{N}(0, \sigma_{z_t}^2)$$

When a time series is in state z_t , its future values evolve according to the autoregressive weights $A_{1,z_t} \cdots A_{r,z_t}$ and noise $e(z_t)$. Since the number of such states in the data is not known in advance, the Beta process is used [22, 48]. A Beta process allows for infinite number of behaviors but encourages sparse representations. Consider, as an example, a model with K behaviors. Each behavior (each column of matrix F) is modeled by a Bernoulli random variable whose parameter is obtained from a Beta distribution (Beta Bernoulli process), i.e.

$$\theta_k \sim \text{Beta}(\alpha/k, 1), k = 1, \dots, K$$

$$F_{nk} \sim \text{Bernoulli}(\theta_k), n = 1, \dots, N \quad (2)$$

The underlying distribution when this process is extended to infinite number of behaviors—i.e., as K tends to infinity—is the Beta process. This process is also known as the *Indian Buffet Process* [19, 28] which can be best understood with the following “culinary metaphor” involving a sequence of customers (time series) selecting dishes (features) from an infinitely large buffet. The n -th customer selects dish k with probability m_k/n , where m_k is the popularity of the dish, i.e., some features are going to be more prevalent than others. S/He then selects

$Poisson(\alpha/n)$ new dishes. With this approach, the number of features can grow arbitrarily with the size n of the dataset: in other words, the feature space increases if the data cannot be faithfully represented with the already defined states. However, the probability of adding new states decreases according to $Poisson(\alpha/n)$. Finally, the distribution generated by the Indian Buffet Process is independent of the order of the customers. For posterior computations the original work is referenced [14, 16].

3.2 Measuring Distance

When applied to multivariate physiological signals, the generative model described above learns a hidden Markov model for each signal. We use the learned HMMs to identify individuals with similar behaviors. In this section we propose two different methods for measuring the distance between HMMs (each HMM represents a participant in the study)

3.2.1 Likelihood Distance: To define a similarity measure between two HMMs, one could measure the probability of their state sequences, having been generated by the same process. Since each signal is associated with its distinct generative process, we measure state sequences' similarity as the likelihood that sequence (S_λ) was generated by λ' , the process that gave rise to ($S_{\lambda'}$), and the likelihood that $S_{\lambda'}$ was generated by λ . We average the two likelihoods to symmetrize the similarity measure.

$$\forall \lambda, \lambda' \text{Sim}(\lambda, \lambda') = \frac{p_{\lambda'}(S_\lambda) + p_\lambda(S_{\lambda'})}{2} \quad (3)$$

The likelihood $p_{\lambda'}(S_\lambda)$ is computed using the learned transition matrix of λ' and Markov process assumption $z_t | z_{t-1} \sim \pi_{z_{t-1}, \lambda'}$, where $\pi_{z_{t-1}, \lambda'}$ is a row of the transition matrix corresponding to state z_{t-1} . Since with this approach longer time series would automatically have a smaller likelihood, we normalize them by dividing $p_{\lambda'}(S_\lambda)$ to $\frac{1}{K}^L$, K being the number of states and L being the length of the time series. Finally since $\pi_{k, \lambda}$ are small probabilities, $\log(\text{Sim}(\lambda, \lambda'))$ is computed which would yield negative similarity values. We negate them to obtain the distance between the time series.

3.2.2 Viterbi Distance: Distance between different HMMs could be also computed with the Viterbi distance proposed in [13]. Viterbi distance is defined as follows:

$$d_{Viterbi}(\lambda, \lambda') = \int_Y \frac{1}{L} \log \frac{p_{\lambda'}(Y, S_{\lambda'})}{p_\lambda(Y, S_\lambda)} P_\lambda(Y) dY \quad (4)$$

Y is any possible time series, L is length of Y , and $p_\lambda(Y, S_\lambda)$ is joint probability of Y and S_λ (state sequence of Y given HMM λ) defined as

$$P_\lambda(Y, S_\lambda) = \max_S P_\lambda(Y, S) \quad (5)$$

Where S in any possible state sequence.

We use the same approximation used in [13] for equation 4 which gives us:

$$d_{Viterbi}^{\sim}(\lambda, \lambda') = \sum_{i,j} a_{ij} \phi_\lambda(i) (\log a'_{ij} - \log a_{ij}) \quad (6)$$

a_{ij} s are the probabilities in transition matrix of λ and $\phi_\lambda(i)$ probability of state i in the stationary distribution of λ . (The stationary distribution will be further explained in section 3.3)

The *Likelihood Distance* computes the distance based on both the state sequences and HMMs, where state sequence is a sample of the HMM (generative) model. The other method, *Viterbi Distance*, computes the values by only comparing the HMMs. This makes Viterbi distance less susceptible to noises observed in state sequences or in other words less sensitive to small changes. This trade-off causes one method to perform better than the other depending on the targeted construct and it's corresponding sensitivity to small variations in the data.

Once the distance between participants is defined, we can perform a number of operations, including learning representations and clustering.

3.3 Learning Representations

In this section we describe two methods for learning representations from the HMMs. The first method is interpretable and could be used for analyzing the data. The second method however gives better performance in predicting most of the constructs.

3.3.1 Stationary Representation: Each HMM is defined by a transition matrix. Transition matrix gives the probability of transitioning from one state to another, so $z_t T_i$ is the probability distribution for z_{t+1} , and $\lim_{x \rightarrow \infty} z_t T_i^x$ is the probability distribution for $\lim_{t \rightarrow \infty} z_t$, which is the stationary distribution. No matter the starting state, the relative amount of time spent in each state is given by the stationary distribution, which is unique for each transition matrix and given by the eigenvector corresponding to the largest eigenvalue of the transition matrix. We use these stationary distributions as features for classification and regression tasks with different models.

3.3.2 Spectral Representation. A drawback of using stationary distribution of the transition matrix to represent participants is that it does not capture the relation between behavioral states, hence it might not be able to distinguish between participants with similar behaviors but which are ordered differently. In order to capture these differences we use distance between participants. Specifically, we perform these steps:

- (1) Calculate the distance matrix between participants using either the likelihood distance or the Viterbi distance described in section 3.2
- (2) Compute the normalized Laplacian of the distance matrix
- (3) Use K largest eigen-vectors (i.e., eigenvectors corresponding to largest eigenvalues) as representations of participants (K is a hyperparameter)

This approach is similar to spectral clustering [50] methods. The intuition behind this approach is that the distance matrix could be interpreted as a weighted adjacency matrix for the network between individuals and the eigen vectors of graph Laplacian provide information about the components and possible cuts in the graph.

4 DATA

The data used in this work comes from an ongoing research study of workplace well-being that measures physical activity, social interactions and physiological states of hospital workers. The study recruited over 200 volunteers from among the employees of a large urban hospital. Participants were enrolled for ten-weeks over the course of three “study waves”, each with different start dates (03/05/18, 04/09/18 and 05/05/18 for waves 1, 2 and 3 respectively). Participants were 31.1% ($n = 66$) male and 68.9% ($n = 146$) female and ranged in age from 21 years to 65 years, with median age of 36 and average of 38.6 years. Most participants were college educated with 59.4% with a Bachelors degree and 21.7% with at least some post-graduate study (Masters or Doctorate). The remaining 18.9% of participants had either a high school diploma or some college. Participants held a variety of job titles: 54.3% were registered nurses, 12% were certified nursing assistants, with the rest reporting some other job title, such as occupational or respiratory therapist, technicians, etc. Overall, two-third of the subjects were nurses. It is worth mentioning that clinical staff in this study works a minimum of 3 days per week (in 12 hour shifts), which can be any day during the week. Nurses exclusively work in day shifts (7am-7pm) or night shifts (7pm-7am). Subjects in other roles can have more flexible work shifts. Depending on the number of workdays during the study, participants wore the sensors for different number of days. Furthermore, participants exhibited varying compliance rates, with a few participants forgetting to wear their sensors on some days. Hence, collected data varies in the amount and length across different participants. Figure 2 shows the distribution of collected data, in

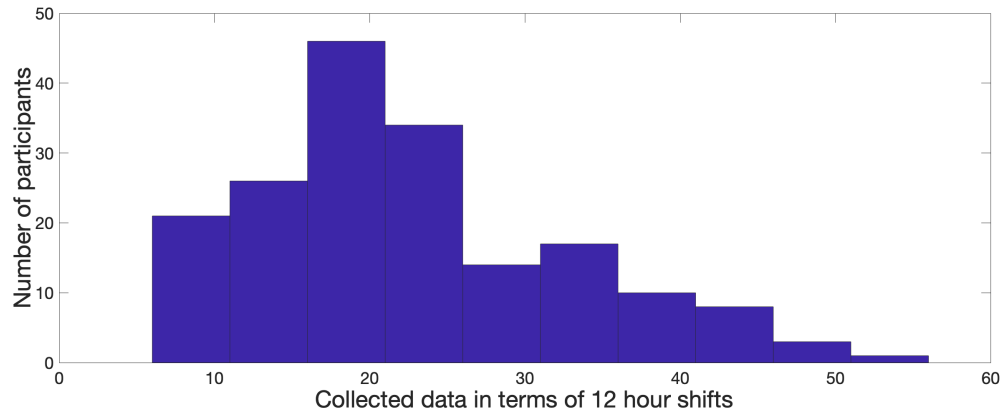


Fig. 2. Histogram of the amount of data collected for the participants. X-axis gives the number of 12-hour shifts and the y-axis gives the number of participants with that many shifts.

terms of 12-hour shifts, over the participants. For this paper, we focused on 180 participants from whom at least 6 days of data was collected.

4.1 Ground Truth Constructs

In addition to wearing sensors, participants were also asked to complete a surveys prior to the study. These pre-study surveys measured job performance, cognitive ability, personality, affect, and health states, which serve as ground truth constructs for our study. Constructs are shown in Table 1. Pre-study surveys also included participant’s demographics such as age, gender, job, etc.

4.2 Sensors and Features

Data used in this paper was collected from a suite of wearable sensors produced by *OMSignal Biometric Smartwear*. These OMSignal garments include sensors embedded in the fabric that measure physiological data in real-time and can relay this information to participant’s smartphone. The OMSignal sensor provides data including heart rate (HR), heart rate variability (HRV), breathing, and accelerometry (to infer sitting position, on-foot movement, and more). Table 2 shows a summary of the sensor signals that we use in this paper. Signal time series all have five min resolution. Participants were instructed to wear OMSignal garments only during their work shifts, although it is hard to verify this.

5 RESULTS

We used BP-AR-HMM with auto regressive lag 1 to model the temporal data collected from sensors worn by the 180 high-compliance participants in the study. For each participant, we constructed vectors representing the 21 features from physiological and movement signals listed in Table 2. We used Z-score to normalize features from sensors. However, since some statistical features like mean and variance are useful for predicting constructs like age, both normalized and unnormalized signals were used in the prediction tasks in Tables 3.

The model identified 23 shared latent states describing participants’ behavior. Some of the states were only exhibited by a few participants. These rare states could convey some useful information that helps identify noise or anomalies in the collected data; however, their sparseness is not beneficial to the prediction and clustering

Table 1. Table of ground truth constructs collected during pre-study surveys.

<i>Name</i>	<i>Description</i>	<i>Instrument</i>
ITP	Job performance	[18]
IRB	In Role Behavior	[54]
IOD-ID	Counter-productive Work behavior	[7]
IOD-OD	Counter-productive Work behavior	[7]
OCB	Organizational Citizenship Behavior	[49]
Shipley Abstraction	Cognitive ability	[43]
Shipley Vocabulary	Cognitive ability	[43]
NEU	Personality: Neuroticism	[17]
CON	Personality: Conscientiousness	[17]
EXT	Personality: Extraversion	[17]
AGR	Personality: Agreeableness	[17]
OPE	Personality: Openness	[17]
POS-AF	Positive affect	[53]
NEG-AF	Negative affect	[53]
STAI	Anxiety	[45]
AUDIT	Alcohol Use Disorders Identification Test	[42]
IPAQ	Physical activity	[33]
PSQI	Sleep quality	[9]
Health limit	Role limitations due to physical health problems	[52]
Emotional limit	Role limitations due to emotional problems	[52]
Well-being	Index of psychological well-being	[52]
Social Functioning	Index of social interaction ability	[52]
Pain	Index of physical pain	[52]
General Health	Index of general health	[52]
Life Satisfaction	Global life satisfaction	[12]
Perceived stress	Perceived stress indicator	[11]
PSY flexibility	Ability to adapt to situational demands	[40]
PSY inflexibility	Inability to adapt to situational demands	[40]
WAAQ	Work-related Acceptance and Action Questionnaire	[8]
Psychological Capital	PCQ a measure of psychological capital	[32]
Challenge Stress	Challenge stress indicator (positive stress)	[39]
Hindrance Stress	Hindrance stress indicator (negative stress)	[39]

tasks. Therefore, we ignore states observed in fewer than 5% of the time series. For example, one of these states observes a constant heart rate which shows a malfunction in the sensor.

5.1 Clustering

For validating the distance measures defined in Section 3.2, we apply hierarchical agglomerative clustering calculated on the distance matrices. As mentioned in 3.2 the likelihood distance is more sensitive to small variations in the data, hence the resulting dendrogram has more structure compared to the dendrogram generated

<i>Signal</i>	<i>Feature</i>
Biometrics: 6 features	Heart Rate, R-R Peak Coverage Avg. Breathing Depth, Avg. Breathing Rate Std. Breathing Depth, Std. Breathing Rate
Movement: 15 features	Intensity, Cadence Steps, Sitting, Supine Avg. G Force, Std. G Force Angle From Vertical, Low G Coverage Avg. X-Acceleration, Std. X-Acceleration Avg. Y-Acceleration, Std. Y-Acceleration Avg. Z-Acceleration, Std. Z-Acceleration

Table 2. Extracted Features from OMSignal.

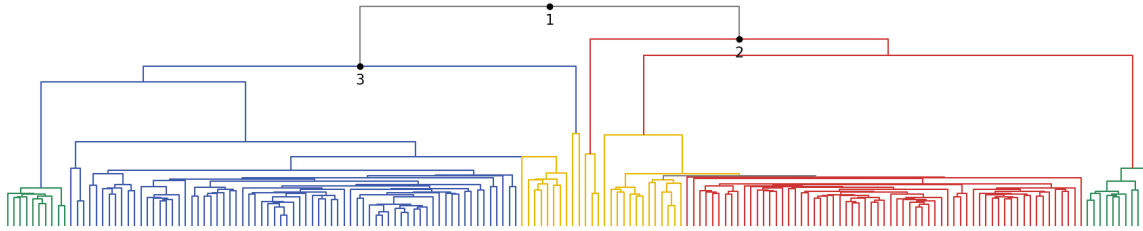


Fig. 3. Dendrogram showing the similarity of participants based on their learned states.

using the Viterbi distance, the groupings of the participants in the dendograms however are very similar in both cases. Therefore we only focus on the dendrogram generated using the likelihood distance, shown in figure 3.

To evaluate the quality of the dendrogram, we used responses gathered from participants during the pre-study surveys and performed statistical tests to evaluate differences between the branches. We partitioned the dendrogram into clusters with more than five members by cutting the dendrogram horizontally on different depths. For continuous-valued labels we performed one-way ANOVA test, a generalization of the T-test for multiple groups, and for categorical labels we performed Kruskal-Wallis H-test with the same setting. Based on the P-values obtained from ANOVA test and Kruskal-Wallis H-test, the most important features differentiating the branches (clusters) were job type, age and gender in that order. This was aligned with our expectations, since different job types require different activities, also age and gender affect physiological signals [30, 56].

The first cut point (marked 1 at the top of Figure 3) separates registered nurses from other jobs types with precision 0.79 and recall 0.70. In other words, 79% of individuals in the red cluster (cluster 2) are registered nurses. The main difference between the two clusters (red and blue) is the frequency of three latent states, which we call **A**, **B** and **C**. In the two states **A** and **B**, the participant was seated, based on the binary sitting signal. Additionally, variables related to acceleration and movement are almost zero for state **A**; however, state **B** is more representative of higher activity levels. Participants in state **B** have higher intensity, cadence, breathing and heart rate. This distinction of participants that are seated while features such as acceleration and steps are non-zero, suggests that these participants are moving around, for example, in a rolling chair. Frequency of state **B** is higher in cluster 2, while frequency of state **A** is higher for participants in cluster 3, and since the majority of individuals in cluster 2 are registered nurses, state **B** could represent activities like checking on patients and moving around while seated, and state **A** represents desk jobs. Figure 4 shows a visualization of these two states.

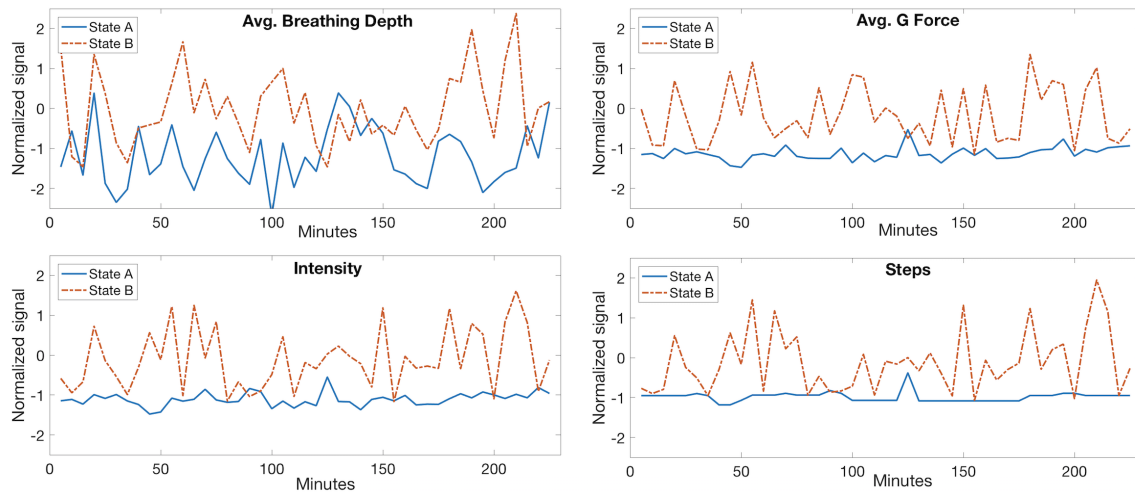


Fig. 4. Comparison of states **A** and **B** using four signals from the same participant. For this plot a segment of signal where the participant was in state **A** and another segment where she was in state **B** is chosen and values coming from the sensors are displayed.

State **C** mostly captures flexibility of work hours for non-nurses (non-nurse participants are more likely to finish their shifts earlier and have less than 12 hours worth of data in one shift).

This clustering can also separate participants based on other demographic information such as work shifts. Work shifts, day or night shifts, are distinguished by state **D**. It will be further described how this is recognized in the prediction section. In this state binary supine signal, which is activated when the participants is lying down, is on. Using only the percentage of time spent in state **D** we can predict day or night shift of participants, with $F1 = 0.68$. It appears that state **D** captures quick naps in the work place and has a higher frequency for night shift participants. Participants who exhibit state **D** are shown by color yellow in Figure 3. There is however another state where the supine variable is on, state **E**. This state has a higher breathing depth and lower movements compared to **D**, and it usually lasts a few hours in a more continuous scenario. Participants with behaviour **E** are shown in Figure 3 with color green. Although participants were asked to wear the sensors while working, they could have kept them on at home, and state **E** may represent a longer night/day sleep at home, rather than at the workplace. Recognizing this, is beneficial for cleaning data even for other models.

5.2 Prediction

We use the learned representations for each participant as features to predict the ground truth constructs. The objective is two-fold: not only do we want to predict, but also, gain understanding about what the latent states represent.

5.2.1 Qualitative Results. Some of the behaviors learned by the model have natural interpretations (states **A** and **B** from Figure 4), while others may be harder to explain. Thus, a possible way to understand latent behaviors is to quantify their importance in explaining constructs. The stationary representation described in section 3.3 has a clear interpretation, with each dimension representing the percentage of time spent in the corresponding state. We explain the behavioral states using the stationary representation with the following process:

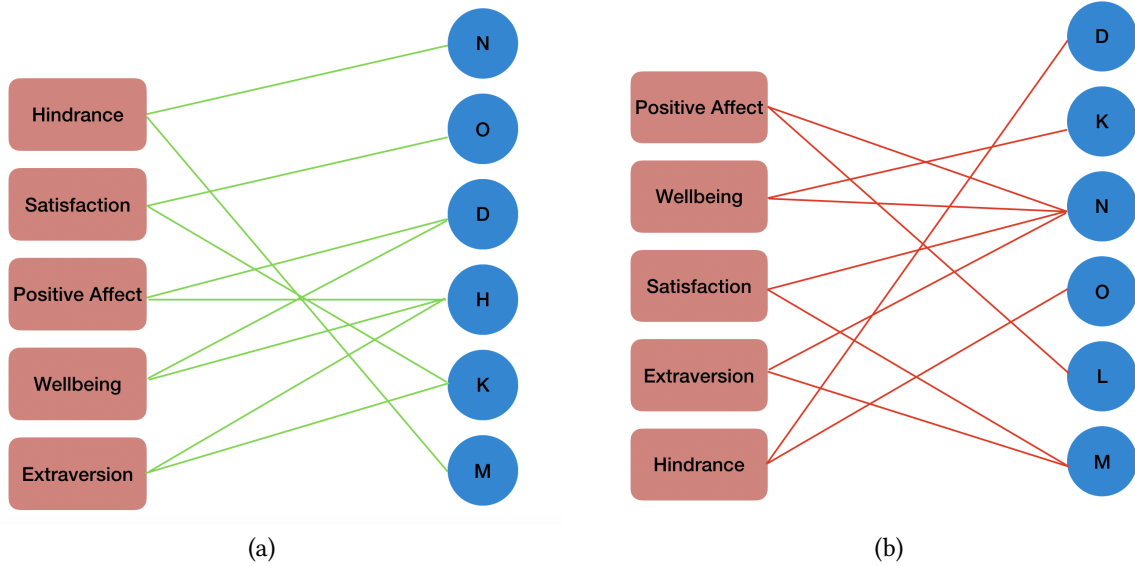


Fig. 5. Bipartite graphs with subset of constructs from Table 1 and subset of states. In (a) each construct is connected to two states whose regression coefficients are the highest (i.e., strongest positive relationship); and in (b) each construct is connected to two states with the lowest negative coefficients (i.e., strongest negative relationship).

- (1) Get the stationary representations of participants
- (2) Run classification/regression on the representations to predict each construct.
- (3) Retrieve the learned coefficients. Each coefficient corresponds to one dimension of the embedding which represents behavioral states.
- (4) Select the states with highest positive and lowest negative coefficients and interpret these states based on their relation with the targeted construct.

Figure 5 shows a subset of constructs and the states that best predict them. Based on this approach we recognized state **D**, described in the section 5.1, as the most relevant state for differentiating between day and night shift employees. State **D** also helps predict positive affect (POS-AF), well-being, and hindrance stress. State **D** has a positive coefficient in predicting POS-AF and Well-being, whereas for hindrance stress it has a negative coefficient. Hindrance stress is generally perceived as a type of stress that prevents progress toward personal accomplishments. Thus, a plausible interpretation of these results is: Quick naps or breaks during work hours could increase positive affect and well-being and decrease hindrance stress. Similarly as shown in Figure 5, state **N** which has a large positive coefficient in predicting hindrance stress, has a large negative coefficient in predicting positive affect, well-being, life satisfaction, and extraversion.

5.2.2 Quantitative Results. For predicting constructs, we used both normalized (z-score) and un-normalized signals as inputs to the BP-AR-HMM and obtained stationary representations and spectral representations using both distance measures (likelihood and Viterbi distance). In this work we refer to method with stationary representation as HMM-S, spectral representation with likelihood distance as HMM-SL and spectral representation with Viterbi distance as HMM-SV. Spectral representation requires a hyperparameter K , number of eigen vectors to include in the representation. We set the K to 10, 20, . . . , 100. We run ridge, kernel ridge and random forest regression on all three learned representations and report the best model. The results are reported in correlation

Table 3. Evaluation of the model on the construct prediction task. The best performing model's results are highlighted in bold.

Construct	ρ	RMSE	ρ	RMSE	ρ	RMSE	ρ	RMSE	ρ	RMSE
	HMM-S		HMM-SL		HMM-SV		RWS		Parafac2	
ITP	-0.729	0.493	0.073	0.488	0.288	0.469	-0.143	0.494	0.105	0.487
IRB	-0.481	4.166	0.193	4.066	0.203	4.055	-0.146	4.18	0.265	4.014
IOD-ID	-0.728	5.185	0.11	5.124	0.136	5.108	-0.534	5.22	-0.709	5.182
IOD-OD	-0.326	6.917	0.202	6.715	0.244	6.634	-0.168	6.891	-0.01	6.864
OCB	0.168	12.035	0.167	12.035	0.245	11.884	0.112	12.159	0.215	11.986
Shipley abstract	0.178	3.732	0.085	3.777	0.179	3.756	0.148	3.764	0.314	3.603
Shipley vocabulary	0.26	4.713	0.085	4.841	0.213	4.748	0.297	4.643	0.399	4.486
NEU	0.066	0.726	0.159	0.718	0.174	0.722	0.048	0.728	0.116	0.724
CON	-0.165	0.62	0.245	0.591	0.181	0.6	-0.033	0.613	0.093	0.612
EXT	0.154	0.655	0.152	0.659	0.264	0.642	0.178	0.65	0.038	0.66
AGR	-0.428	0.491	0.122	0.485	0.191	0.479	0.079	0.488	0.099	0.488
OPE	0.224	0.586	0.217	0.581	0.28	0.571	0.216	0.585	-0.386	0.598
POS-AF	0.37	6.547	0.254	6.614	0.231	6.686	0.139	6.821	0.112	6.822
NEG-AF	-0.278	5.293	0.235	5.139	0.206	5.195	0.045	5.286	0.139	5.238
STAI	0.016	8.975	0.196	8.817	0.112	8.919	0.128	8.912	0.095	8.966
AUDIT	0.1	2.159	0.362	2.017	0.153	2.142	0.053	2.169	0.244	2.113
IPAQ	-0.57	15352	0.094	15191	0.115	15316	0.033	15311	0.097	15246
PSQI	-0.682	2.366	0.178	2.318	0.142	2.33	0.193	2.322	0.194	2.311
Age	0.461	8.613	0.091	9.662	0.084	9.667	0.243	9.406	0.363	9.035
Health Limit	-0.75	23.284	0.196	22.704	0.333	21.986	0.222	23.325	0.118	23.264
Emotional Limit	-0.704	22.71	0.211	22.102	0.164	22.504	0.042	22.652	0.091	22.553
Well being	0.077	18.458	0.152	18.302	0.276	17.904	0.011	18.682	0.167	18.277
Social Functioning	0.057	21.94	0.109	21.684	0.191	21.547	0.085	21.857	0.218	21.541
Pain	0.167	18.613	0.134	18.448	0.239	18.164	0.023	18.658	0.102	18.571
General Health	0.211	17.062	0.27	16.792	0.171	17.28	0.151	17.311	0.2	17.105
Life Satisfaction	-0.655	1.354	0.106	1.338	0.22	1.317	-0.125	1.362	0.207	1.317
Perceived Stress	0.196	0.511	0.201	0.51	0.209	0.511	0.195	0.513	-0.728	0.524
PSY flexibility	-0.793	0.821	0.187	0.806	0.233	0.795	-0.077	0.823	0.103	0.813
PSY inflexibility	-0.66	0.803	0.182	0.785	0.152	0.79	-0.013	0.803	0.006	0.8
WAAQ	0.31	5.65	0.284	5.705	0.205	5.833	0.153	5.878	0.163	5.866
Psychological Capital	0.188	0.656	0.129	0.661	0.17	0.662	0.12	0.662	0.08	0.664
Challenge Stress	-0.639	0.622	0.171	0.615	0.078	0.62	-0.097	0.623	-0.789	0.621
Hindrance Stress	0.132	0.644	0.005	0.646	0.206	0.633	0.035	0.647	0.143	0.637

to the target construct (ρ) and Root Mean Squared Error (RMSE) using Leave-one-out cross validation Table 3 shows results of the regression task.

5.2.3 Baselines. We compare our results against *Random Warping Series (RWS)*[55] and *Parafac2* [21]. RWS is the state-of-the-art method for time series embedding. This method constructs kernels over features extracted from time series. Extracted features are given by Dynamic Time Warping, an algorithm that is used for measuring

the similarity between a number of randomly generated sequences and the original sequence. This method has three hyperparameters: R , D and σ . The first parameter, R , specifies the size of the embedding and number of random time-series generated to be compared with the original time series. Parameter D is the length of the random time series generated and σ is the choice of the kernel parameter. Based on authors suggestion, we fixed the value of R to a large number, 512 based on their implementation, and experimented with few different values for D and σ . This means that the embeddings generated were in a 512 dimensional space.

We use similar techniques—ridge, kernel ridge and random forest regression – on the embeddings learned by different hyperparameters and compare the best results with our own results. This also holds for the next baseline Parafac2.

The second baseline we use is *Parafac2* [21]. This approach views the data as a tensor (3 dimensional array) of participants-sensors-time and decomposes it into hidden components by applying SVD to the multivariate time series for each user, while sharing the same factors across variable dimensions, e.g. heart rate, breathing rate. These vectors could be interpreted as level of involvement in the hidden component: i.e., the vector along the dimension of number of participants shows the intensity of that hidden factor for each individual which can be used as features for regression or classification. For Parafac2 the number of hidden components must be given in advance. We varied the number of hidden components from one to ten and also used both normalized and un-normalized signals as inputs to the model and report the best result based on ρ and RMSE in Table 3.

Overall, the results of the predictions based on the HMM's latent states were systematically better, outperforming the baseline method in 28 out of the 33 constructs predicted. It's worth mentioning that except for HMM-S which is non-parametric, all other four models in Table 3 have hyperparameters that need to be set. We tune the hyperparameters by running 10 different settings and selecting the setting with best results. This might be the reason why RWS is not performing as well. Because it has three hyperparameters while the other models (except for HMM-S) have one hyperparameter hence it needs more tuning compared to the other models.

Between our own representations (HMM-S, HMM-SL, HMM-SV), HMM-SV performs better for some construct while HMM-SL gives better results for others. This could be because of the differences between Viterbi and likelihood distance and their sensitivity to small variations in the data, discussed more in section 3.2. Also HMM-S is not a good representation for prediction and is better suited for analysis of the data.

6 CONCLUSION

In this work, we described a method for learning behavioral representations from dynamic physiological data captured by wearable sensors using a Bayesian non-parametric framework that combines *Hidden Markov Models* and the *Beta Process*. This method can overcome limitations of state-of-the-art alternatives, including handling unaligned time series with different lengths, robust inference with missing data and noise, and finally discovery of dynamic behaviors without any *a priori* knowledge about the behavioral states to be identified. We used this model to learn behavioral representations for data collected from workers of a large urban hospital. The 200 volunteers were enrolled in a 10-week long study and were asked to wear a suite of sensors.

The latent states learned by the model capture behavioral differences within the population and can also be used to predict their self-reported health and psychological well-being. In comparison to alternative models, our framework improves performance with compact representations of the multivariate time-series; leading to less overfitting and easier interpretation of the states learned. Concluding, we show that this framework can also cluster study participants into meaningful, cohesive groups exhibiting similar behaviors and characteristics.

This work can be extended in a number of ways. One possible direction is making this framework supervised. Using this framework as is, helps in analyzing multivariate signals and although learned states can predict some constructs very well, making this framework supervised could be more suited for a prediction task.

7 ACKNOWLEDGEMENT

The authors are grateful to the TILES team for the efforts in study design, data collection and sharing, that enable this work. This research is based upon work supported by the Office of the Director of National Intelligence (ODNI), Intelligent Advanced Research Projects Activity (IARPA), via IARPA Contract No 2017-17042800005. The views and conclusions contained herein are those of the authors and should not be interpreted as necessarily representing the official policies or endorsements, either expressed or implied, of the ODNI, IARPA, or the U.S. Government. The U.S. Government is authorized to reproduce and distribute reprints for Governmental purposes notwithstanding any copyright annotation thereon.

REFERENCES

- [1] Laure Amate, Florence Forbes, Julie Fontecave-Jallon, Benoît Vettier, and Catherine Garbay. 2011. Probabilistic model definition for physiological state monitoring. In *Statistical Signal Processing Workshop (SSP), 2011 IEEE*. IEEE, 457–460.
- [2] Charles E Antoniak. 1974. Mixtures of Dirichlet processes with applications to Bayesian nonparametric problems. *The annals of statistics* (1974), 1152–1174.
- [3] Sinan Aral and Christos Nicolaides. 2017. Exercise contagion in a global social network. *Nature communications* 8 (2017), 14753.
- [4] Ling Bao and Stephen S Intille. 2004. Activity recognition from user-annotated acceleration data. In *International conference on pervasive computing*. Springer, 1–17.
- [5] Leonard E Baum and Ted Petrie. 1966. Statistical inference for probabilistic functions of finite state Markov chains. *The annals of mathematical statistics* 37, 6 (1966), 1554–1563.
- [6] Matthew J Beal, Zoubin Ghahramani, and Carl E Rasmussen. 2002. The infinite hidden Markov model. In *Advances in neural information processing systems*. 577–584.
- [7] Christopher M Berry, Deniz S Ones, and Paul R Sackett. 2007. Interpersonal deviance, organizational deviance, and their common correlates: A review and meta-analysis. *Journal of applied psychology* 92, 2 (2007), 410.
- [8] Frank W Bond, Joda Lloyd, and Nigel Guenole. 2013. The work-related acceptance and action questionnaire: Initial psychometric findings and their implications for measuring psychological flexibility in specific contexts. *Journal of Occupational and Organizational Psychology* 86, 3 (2013), 331–347.
- [9] Daniel J Buysse, Charles F Reynolds III, Timothy H Monk, Susan R Berman, and David J Kupfer. 1989. The Pittsburgh Sleep Quality Index: a new instrument for psychiatric practice and research. *Psychiatry research* 28, 2 (1989), 193–213.
- [10] Jeremy E Cohen and Rasmus Bro. 2018. Nonnegative PARAFAC2: a flexible coupling approach. In *International Conference on Latent Variable Analysis and Signal Separation*. Springer, 89–98.
- [11] Sheldon Cohen, T Kamarck, R Mermelstein, et al. 1994. Perceived stress scale. *Measuring stress: A guide for health and social scientists* (1994), 235–283.
- [12] ED Diener, Robert A Emmons, Randy J Larsen, and Sharon Griffin. 1985. The satisfaction with life scale. *Journal of personality assessment* 49, 1 (1985), 71–75.
- [13] Markus Falkhausen, Herbert Reininger, and Dietrich Wolf. 1995. Calculation of distance measures between hidden Markov models. In *Fourth European Conference on Speech Communication and Technology*.
- [14] Emily Fox, Michael I Jordan, Erik B Sudderth, and Alan S Willsky. 2009. Sharing features among dynamical systems with beta processes. In *Advances in Neural Information Processing Systems*. 549–557.
- [15] Emily Fox, Erik B Sudderth, Michael I Jordan, and Alan S Willsky. 2009. Nonparametric Bayesian learning of switching linear dynamical systems. In *Advances in Neural Information Processing Systems*. 457–464.
- [16] Emily B Fox, Michael C Hughes, Erik B Sudderth, Michael I Jordan, et al. 2014. Joint modeling of multiple time series via the beta process with application to motion capture segmentation. *The Annals of Applied Statistics* 8, 3 (2014), 1281–1313.
- [17] Samuel D Gosling, Peter J Rentfrow, and William B Swann Jr. 2003. A very brief measure of the Big-Five personality domains. *Journal of Research in personality* 37, 6 (2003), 504–528.
- [18] M. Griffin, A. Neal, and S. Parker. 2007. A new model of work role performance: positive behavior in uncertain and interdependent contexts. *Academy of Management Journal* 50, 2 (2007), 327–347.
- [19] Thomas L Griffiths and Zoubin Ghahramani. 2011. The indian buffet process: An introduction and review. *Journal of Machine Learning Research* 12, Apr (2011), 1185–1224.
- [20] David Hallac, Sagar Vare, Stephen Boyd, and Jure Leskovec. 2017. Toeplitz inverse covariance-based clustering of multivariate time series data. In *Proceedings of the 23rd ACM SIGKDD International Conference on Knowledge Discovery and Data Mining*. ACM, 215–223.
- [21] Richard A Harshman. 1970. Foundations of the PARAFAC procedure: Models and conditions for an “explanatory” multimodal factor analysis. (1970).

- [22] Nils Lid Hjort et al. 1990. Nonparametric Bayes estimators based on beta processes in models for life history data. *The Annals of Statistics* 18, 3 (1990), 1259–1294.
- [23] Homa Hosseinmardi, Amir Ghasemian, Shrikanth Narayanan, Kristina Lerman, and Emilio Ferrara. 2018. Tensor Embedding: A Supervised Framework for Human Behavioral Data Mining and Prediction. *arXiv preprint arXiv:1808.10867* (2018).
- [24] Homa Hosseinmardi, Hsien-Te Kao, Kristina Lerman, and Emilio Ferrara. 2018. Discovering hidden structure in high dimensional human behavioral data via tensor factorization. In *WSDM Heteronam Workshop*.
- [25] Joseph W Houpt, Mary E Frame, and Leslie M Blaha. 2018. Unsupervised parsing of gaze data with a beta-process vector auto-regressive hidden Markov model. *Behavior research methods* 50, 5 (2018), 2074–2096.
- [26] Philip JH Jørgensen, Søren FV Nielsen, Jesper L Hinrich, Mikkel N Schmidt, Kristoffer H Madsen, and Morten Mørup. 2018. Probabilistic PARAFAC2. *arXiv preprint arXiv:1806.08195* (2018).
- [27] Eamonn Keogh, Kaushik Chakrabarti, Michael Pazzani, and Sharad Mehrotra. 2001. Dimensionality reduction for fast similarity search in large time series databases. *Knowledge and information Systems* 3, 3 (2001), 263–286.
- [28] John Kingman. 1967. Completely random measures. *Pacific J. Math.* 21, 1 (1967), 59–78.
- [29] Tamara G Kolda and Brett W Bader. 2009. Tensor decompositions and applications. *SIAM review* 51, 3 (2009), 455–500.
- [30] Andreas Lanitis. 2009. A survey of the effects of aging on biometric identity verification. *International Journal of Biometrics* 2, 1 (2009), 34–52.
- [31] Jessica Lin, Eamonn Keogh, Stefano Lonardi, and Bill Chiu. 2003. A symbolic representation of time series, with implications for streaming algorithms. In *Proceedings of the 8th ACM SIGMOD workshop on Research issues in data mining and knowledge discovery*. ACM, 2–11.
- [32] Fred Luthans, Bruce J Avolio, James B Avey, and Steven M Norman. 2007. Positive psychological capital: Measurement and relationship with performance and satisfaction. *Personnel psychology* 60, 3 (2007), 541–572.
- [33] R. Maddison, C. Ni Mhurchu, Y. Jiang, S. Vander Hoorn, A. Rodgers, C. Lawes, and E. Rush. 2007. International Physical Activity Questionnaire (IPAQ) and New Zealand Physical Activity Questionnaire (NZPAQ): A doubly labelled water validation. *Int. Journal of Behavioral Nutrition and Physical Activity* 4, 1 (2007), 62.
- [34] Valérie Monbet and Pierre Ailliot. 2017. Sparse vector Markov switching autoregressive models. Application to multivariate time series of temperature. *Computational Statistics & Data Analysis* 108 (2017), 40–51.
- [35] Daniel Novak, Lenka Lhotska, T Al-Ani, Y Hamam, D Cuesta-Frau, P Micó, and Mateo Aboy. 2004. Morphology analysis of physiological signals using hidden Markov models. In *Pattern Recognition, 2004. ICPR 2004. Proceedings of the 17th International Conference on*, Vol. 3. IEEE, 754–757.
- [36] Emma Pierson, Tim Althoff, and Jure Leskovec. 2018. Modeling Individual Cyclic Variation in Human Behavior. In *Proceedings of the 2018 World Wide Web Conference on World Wide Web*. International World Wide Web Conferences Steering Committee, 107–116.
- [37] Lawrence R Rabiner and Biing-Hwang Juang. 1986. An introduction to hidden Markov models. *ieee assp magazine* 3, 1 (1986), 4–16.
- [38] Nishkam Ravi, Nikhil Dandekar, Preetham Mysore, and Michael L Littman. 2005. Activity recognition from accelerometer data. In *Aaai*, Vol. 5. 1541–1546.
- [39] Jessica B Rodell and Timothy A Judge. 2009. Can “good” stressors spark “bad” behaviors? The mediating role of emotions in links of challenge and hindrance stressors with citizenship and counterproductive behaviors. *Journal of Applied Psychology* 94, 6 (2009), 1438.
- [40] Ronald Rogge. 2016. The Multidimensional Psychological Flexibility Inventory (MPFI). <https://doi.org/10.13140/RG.2.1.1645.9129>
- [41] Anna Sapienza, Alessandro Bessi, and Emilio Ferrara. 2018. Non-negative tensor factorization for human behavioral pattern mining in online games. *Information* 9, 3 (2018), 66.
- [42] J. B. Saunders, O. G. Asaland, T. F. Babor, J. R. De la Fuente, and M. Grant. 1993. Development of the Alcohol Use Disorders Identification Test (AUDIT): WHO collaborative project on early detection of persons with harmful alcohol consumption. *Addiction* 89, 6 (1993).
- [43] W. C. Shipley, C. P. Gruber, T. A. Martin, and A. M. Klein. 2009. *Shipley-2 Manual*. Western Psychological Service, Los Angeles, CA.
- [44] Abhishhek Singh, Tejaswi Tamminedi, Guy Yosiphon, Anurag Ganguli, and Jacob Yadegar. 2010. Hidden Markov Models for modeling blood pressure data to predict acute hypotension. In *Acoustics Speech and Signal Processing (ICASSP), 2010 IEEE International Conference on*. IEEE, 550–553.
- [45] C. D. Spielberger, G. A. Jacobs, S. Russell, and R. S. Crane. 1983. Assessment of anger: The State-Trait Anger Scale. In *Advances in Personality Assessment*. Erlbaum, Hillsdale, New Jersey.
- [46] Emmanuel Munguia Tapia, Stephen S Intille, and Kent Larson. 2004. Activity recognition in the home using simple and ubiquitous sensors. In *International conference on pervasive computing*. Springer, 158–175.
- [47] Nazgol Tavabi, Nathan Bartley, Andrés Abeliuk, Sandeep Soni, Emilio Ferrara, and Kristina Lerman. 2019. Characterizing Activity on the Deep and Dark Web. *arXiv preprint arXiv:1903.00156* (2019).
- [48] Romain Thibaux and Michael I Jordan. 2007. Hierarchical beta processes and the Indian buffet process. In *Artificial Intelligence and Statistics*. 564–571.
- [49] Linn Van Dyne, Jill W Graham, and Richard M Dienesch. 1994. Organizational citizenship behavior: Construct redefinition, measurement, and validation. *Academy of management Journal* 37, 4 (1994), 765–802.

- [50] Ulrike Von Luxburg. 2007. A tutorial on spectral clustering. *Statistics and computing* 17, 4 (2007), 395–416.
- [51] Rui Wang, Fanglin Chen, Zhenyu Chen, Tianxing Li, Gabriella Harari, Stefanie Tignor, Xia Zhou, Dror Ben-Zeev, and Andrew T Campbell. 2014. StudentLife: assessing mental health, academic performance and behavioral trends of college students using smartphones. In *Proceedings of the 2014 ACM international joint conference on pervasive and ubiquitous computing*. ACM, 3–14.
- [52] John E Ware Jr and Cathy Donald Sherbourne. 1992. The MOS 36-item short-form health survey (SF-36): I. Conceptual framework and item selection. *Medical care* (1992), 473–483.
- [53] David Watson, Lee Anna Clark, and Auke Tellegen. 1988. Development and validation of brief measures of positive and negative affect: the PANAS scales. *Journal of personality and social psychology* 54, 6 (1988), 1063.
- [54] L. J. Williams and S. E. Anderson. 1991. Job satisfaction and organizational commitment as predictors of organizational citizenship and in-role behaviors. *J. of Management* 17, 3 (1991), 601–617.
- [55] Lingfei Wu, Ian En-Hsu Yen, Jinfeng Yi, Fangli Xu, Qi Lei, and Michael Witbrock. 2018. Random warping series: a random features method for time-series embedding. *arXiv preprint arXiv:1809.05259* (2018).
- [56] Yingxiao Wu, Yan Zhuang, Xi Long, Feng Lin, and Wenyao Xu. 2015. Human gender classification: A review. *arXiv preprint arXiv:1507.05122* (2015).